Auszug aus: Proc. of the 5 th Int. COPEDEC, Cape Town, South Africa, 1999

APPLICABILITY OF WAVE MODELS IN SHALLOW COASTAL WATERS

by

Stephan Mai[1+] , Nino Ohle[2+] and Claus Zimmermann[3+]

ABSTRACT

The wave propagation within coastal areas is strongly influenced by the coastal morphology with its islands, bars, shoals and channels. Predominant processes in this zone are shoaling, bottom friction, breaking, refraction, wind generation and to some extent diffraction of waves. The numerical formulation of these processes in standard wave models, like HISWA (HIndcast Shallow Water WAves, TU Delft), SWAN (Simulation WAves Nearshore, TU Delft) and MIKE 21 EMS (Elliptic Mild Slope, Danish Hydraulic Institute) were tested by comparing the simulation results with measurements in a wave tank and on site measurements at the North Frisian Coast of Germany. The numerical and experimental data measured in the wave flume are in very good agreement for all applied wave models proving the numerical formulation quality of bottom friction, shoaling and breaking. A comparison of numerical simulations results with SWAN and field data shows also a quite good agreement but revealed in some cases larger differences which may be contributed to the interaction of tidal currents and waves.

1. INTRODUCTION

Due to the complexity of wave propagation in coastal areas the estimation of wave parameters for engineering purposes is based on numerical simulations. In contrast to the ray tracing technique of conventional wave models which often lead to chaotic wave ray patterns and therefore to a difficult interpretation the numerical formulation of basic wave equations on a regular grid becomes more common (Ris et al., 1994). Examples for wave models with regular grids are the standard models HISWA (Booij et al., 1985), SWAN (Ris, 1997) and MIKE 21 EMS (Madsen and Larsen, 1987). These wave models differ in the set of basic equations and the mathematical formulation employed to describe e.g. bottom friction, wave breaking and wind generation. Experiments in the large wave tank of FORSCHUNGSZENTRUM KÜSTE, Hannover, Germany, on the wave propagation along a foreland with submerged dike are used to test the applicability of these wave models in shallow waters putting emphasis on the adjustment of the parameter of bottom friction and wave breaking. Similar model tests are described for HISWA by Booij et al. (1985), by Mai et al. (1998) or by Kaiser and Niemeyer (1998) and for SWAN by Ris (1997). Based on field measurements of the public department ALR Husum, Germany, at the North Frisian wadden sea coast additional tests of SWAN are presented using the standard setting of model parameters. Analogous comparisons are given by Ris (1997) or by Kaiser and Niemeyer (1998).

[1] Stephan.Mai@fi.uni-hannover.de

[2] Nino.Ohle@fi.uni-hannover.de

[3] Claus.Zimmermann@fi.uni-hannover.de

[+] University of Hannover, Franzius-Institut, Nienburger Str. 4, 30167 Hannover, Germany

2. WAVE MODELS

2.1 Basic Model Equations

The wave model HISWA and the advanced model SWAN are based on the following action balance equation:

$$\frac{\partial}{\partial t}N_{(x,y,\sigma,\theta)} + \frac{\partial}{\partial x}c_x N_{(x,y,\sigma,\theta)} + \frac{\partial}{\partial y}c_y N_{(x,y,\sigma,\theta)} + \frac{\partial}{\partial \sigma}c_\sigma N_{(x,y,\sigma,\theta)} + \frac{\partial}{\partial \theta}c_\theta N_{(x,y,\sigma,\theta)} = \frac{S_{(x,y,\sigma,\theta)}}{\sigma} \qquad (1)$$

where the geographical coordinates are x and y, the propagation direction is θ, the relative frequency is $\sigma = \omega - \bar{k}\cdot\bar{u}$, the wave number is $\bar{k}$, the depth-averaged underlying current is $\bar{u}$, the action density spectrum is $N_{(x,y,\sigma,\theta)} = E_{(x,y,\sigma,\theta)}/\sigma$, the propagation velocities are c_x, c_y, c_σ, c_θ of wave energy in geographical and spectral space and the energy source term is $S_{(x,y,\sigma,\theta)}$ (Ris, 1997, Holthuijsen and Booij, 1987).

The processes of shoaling and refraction are implied in the left hand side of equation 1 by the definition of propagation velocities $\bar{c} = (c_x, c_y)$ as the sum of group velocity $\bar{c}_g$ and underlying current:

$$\bar{c} = \bar{c}_g + \bar{u} = \frac{1}{2}\left(1 + \frac{2\cdot k\cdot d}{\sinh(2\cdot k\cdot d)}\right)\frac{\sigma\cdot\bar{k}}{k^2} + \bar{u} \qquad (2)$$

in which d is the water depth.

The influence of currents on wave propagation is not taken into consideration within our model tests, i.e. $|\bar{u}| = 0$.

The processes of dissipation of wave energy due to water-depth induced breaking $S_{ds,br}$ or wave bottom interactions $S_{ds,b}$ and the generation of wave energy by wind S_{in} are included in the energy source term:

$$S_{(x,y,\sigma,\theta)} = S_{ds,br} + S_{ds,b} + S_{in} + ... \qquad (3)$$

Diffraction is not described by the action balance equation and therefore not included in HISWA and SWAN. The time-dependence of the action balance equation is neglected in our model test of HISWA and SWAN although SWAN contains a non-stationary mode.

The action balance equation is solved in SWAN with a full discrete two-dimensional wave-spectrum $N_{(x,y,\sigma,\theta)}$ using an iterative four-sweep technique allowing wave-propagation in all directions in the entire geographical domain. In contrast to this the wave spectrum in HISWA is discrete only in directions but parametric in frequency, i.e. the shape of the frequency spectrum is prescribed. This prescription of shape is especially problematic in case of double-peaked spectra. Using the parametric frequency spectrum the action balance equation (eq. 1) is separated into evolution equations for the zero-order moment and the first-order moment of action-density spectrum. The evolution equations in HISWA are solved using a forward stepping procedure in the numerical scheme allowing wave propagation in forward direction only.

The wave model MIKE 21 EMS is based on the elliptic mild slope equation:

$$\nabla(c\, c_g\, \nabla\zeta) - \frac{c_g}{c}\frac{\partial^2\zeta}{\partial t^2} = 0 \tag{4}$$

where the phase velocity is $c = \omega \cdot k$ and the surface elevation is ζ (Madsen and Larsen, 1987). Equation 4 includes the processes of refraction, shoaling and diffraction.

In order to include energy dissipation due to bed friction, wave breaking and energy loss inside porous structures in MIKE 21 EMS, the equation 4 is rewritten by introducing complex harmonic pseudo-fluxes P, Q (DHI, 1996):

$$\begin{aligned}
&\frac{c_g}{c}\frac{\partial S}{\partial t} + \left(\frac{c_g}{c}\cdot i\cdot\omega + f_s\right)\cdot S + \frac{\partial P}{\partial x} + \frac{\partial Q}{\partial y} = SS \\
&\frac{c_g}{c}\frac{\partial P}{\partial t} + \left(\frac{c_g}{c}\cdot(i\cdot\omega + \omega\cdot f_p) + f_s + e_f + e_b\right)\cdot P + c_g^2\frac{\partial S}{\partial x} = 0 \\
&\frac{c_g}{c}\frac{\partial Q}{\partial t} + \left(\frac{c_g}{c}\cdot(i\cdot\omega + \omega\cdot f_p) + f_s + e_f + e_b\right)\cdot Q + c_g^2\frac{\partial S}{\partial y} = 0
\end{aligned} \tag{5}$$

where S is the wave amplitude, i is the imaginary unit, f_s and f_p are linear friction factors due to energy loss in an absorbing sponge layer or inside a porous structure and e_f and e_b are factors of energy dissipation due to bed friction and wave breaking.

Wave spectra are parameterized in MIKE 21 using the rms-value of wave height H_{rms} and the peak period T_p. The set of equations 5 is then solved for regular waves with a height of H_{rms} and a period of T_p.

2.2 Dissipation of Wave-Energy due to Bottom Friction

The dissipation of wave energy due to bottom friction is determined in all tested models using a quadratic friction law. In HISWA and SWAN the formulation of this bottom friction model is expressed in the following form:

HISWA: $$S_{ds,b(x,y,\theta)} = -C_{bot}\frac{\sigma_0^2}{g^2\cdot\sinh^2(k_0\cdot d)}E_{(x,y,\theta)} \tag{6}$$

SWAN: $$S_{ds,b(x,y,\sigma,\theta)} = -C_{bot}\frac{\sigma^2}{g^2\cdot\sinh^2(k\cdot d)}E_{(x,y,\sigma,\theta)} \tag{7}$$

where k_0 and σ_0 are the mean wave number and mean wave frequency and C_{bot} is the friction coefficient.

The bottom friction coefficient is a constant model parameter in HISWA. Besides that the bottom friction formulations of Collins (1972) and of Madsen et al. (1988) are included in SWAN:

Collins: $$C_{bot} = C_{fw}\cdot g\cdot u_{rms} \quad \text{and} \quad u_{rms} = \iint\frac{\sigma^2}{\sinh^2(k\cdot d)}E_{(x,y,\sigma,\theta)}d\sigma d\theta \tag{8}$$

Madsen: $$C_{bot} = f_{wr} \cdot \frac{g}{\sqrt{2}} \cdot u_{rms}\,,\ \frac{1}{4\sqrt{f_{wr}}} + \lg\left(\frac{1}{4\sqrt{f_{wr}}}\right) = m_f + \lg\left(\frac{a_b}{K_N}\right) \qquad (9)$$

$$a_b^2 = \iint \frac{1}{\sinh^2(k \cdot d)} E_{(x,y,\sigma,\theta)} d\sigma d\theta$$

in which u_{rms} is the orbital velocity at the bottom, K_N is the equivalent Nikuradse bottom roughness, a_b is a representative near-bottom excursion amplitude, C_{fw}, f_{wr} and m_f are model parameter.

In MIKE 21 EMS the friction model of Dingemans (1983) is used to calculate the dissipation rate per unit area D_b:

$$D_b = \frac{f_e}{16 \cdot \pi \cdot g}\left(\frac{\omega \cdot H_{rms}}{\sinh(k \cdot d)}\right)^3,\ f_e = \begin{cases} 0.24 & ,\ a_b / K_N < 2 \\ \exp\left(-5.977 + 5.213 \cdot \left(\frac{a_b}{K_N}\right)^{-0.194}\right) & ,\ a_b / K_N \geq 2 \end{cases} \qquad (10)$$

$$\text{and } e_f \propto D_b / E \qquad (11)$$

in which $E = \rho \cdot g \cdot H_{rms}^2 / 8$ is the energy density of the wave field and f_e is an energy loss factor.

2.3 Dissipation of Wave-Energy due to Wave Breaking

The numerical formulation of wave breaking is described in all of the models mentioned above according to Battjes and Janssen (1978):

$$D_{br} = \frac{\alpha}{4} Q_b \bar{f} \rho g H_{max}^2 \quad , \quad \frac{1 - Q_b}{\ln Q_b} = -\left(\frac{H_{rms}}{H_{max}}\right)^2 \quad , \quad H_{max} = \frac{\gamma_1}{k}\tanh\left(\frac{\gamma_2}{\gamma_1} k \cdot d\right) \qquad (12)$$

in which D_{br} is the mean dissipation rate per area, Q_b is the fraction of breaking waves, ρ the water density, H_{rms} is the root mean square, H_{max} is the maximum wave height and α, γ_1, γ_2 are adjustable coefficients.

In HISWA and SWAN the total dissipation rate D is assigned to the dissipation rate for each spectral component (Booij et al., 1985, and Ris , 1997):

HISWA: $$S_{ds,br(x,y,\theta)} = -D_{br} \cdot \frac{E_{(x,y,\theta)}}{E_{tot(x,y)}}\ ,\ \text{where}\ \ E_{tot(x,y)} = \int E_{(x,y,\theta)} d\theta \qquad (13)$$

SWAN: $$S_{ds,br(x,y,\sigma,\theta)} = -D_{br} \cdot \frac{E_{(x,y,\sigma,\theta)}}{E_{tot(x,y)}}\ ,\ \text{where}\ \ E_{tot(x,y)} = \iint E_{(x,y,\sigma,\theta)} d\sigma d\theta \qquad (14)$$

In MIKE 21 EMS the dissipation rate is used to calculate the factor of energy dissipation $e_b \propto D_{br} / E$.

2.4 Generation of Wave Energy due to Wind

The wind input of wave energy $S_{in(x,y,\sigma,\theta)}$ is calculated within SWAN using the first-generation mode (Ris, 1997):

$$S_{in(x,y,\sigma,\theta)} = A + B \cdot E_{(x,y,\sigma,\theta)}, \text{ where } B = \max\left(0, \frac{\rho_a}{4 \cdot \rho_w}\left(28 \frac{\sqrt{C_{D,10} \cdot U_{10}^2}}{c} \cos\left(\theta - \theta_w\right) - 1\right)\right) \cdot \sigma \quad (15)$$

$$\text{and } A = \frac{0.0015}{2 \cdot \pi \cdot g^2}\left(\sqrt{C_{D,10} \cdot U_{10}^2} \cdot \max\left(0, \cos\left(\theta - \theta_w\right)\right)\right)^4 \exp\left(-\left(\frac{\sigma}{0.13 \cdot g \cdot 2 \cdot \pi / 28 \cdot \sqrt{C_{D,10} \cdot U_{10}^2}}\right)^{-4}\right) \quad (16)$$

in which $C_{D,10}$ is the drag coefficient, U_{10} is the wind velocity, ρ_A and ρ_W are the air and water density and θ_W is the wind direction.

3. NUMERICAL SIMULATIONS COMPARED TO PHYSICAL MODELING

The experimental data on which the model test presented in this paper is based were collected during an investigation on the influence of summer dikes, i.e. submerged dikes, on waves propagating along a foreland.

For this reason a model of a foreland with summer dike of typical height and width was build at prototype scale in the large wave tank (324 m length, 5 m width and 7 m depth) of the FORSCHUNGSZENTRUM KÜSTE. See for details at Mai (1998). The graph at the bottom of Figure 1 shows a cross section of the foreland profile. The height of the foreland in the wave tank was approximately 1.5 m corresponding to a height of 2.0 m above German datum. The crest height of the summer dike was 3.0 m or 3.5 m above German datum respectively. Its crest width was 3.0 m. The slope was approximately 1:7. The foreland length in seeward direction of the summer dike is approximately 40 m. The polder length in landward direction was about 70 m. The summer dike consists of a sand core protected from erosion by a concrete filled geotextile mattress simulating a clay cover with grass as applied in nature while the foreland was build of sand without any cover. The boundary conditions were varied in a range typical at the German North-Sea coast (water-level: 3.5 m to 4.5 m, i.e. 4.0 m to 5.0 m above German datum, significant wave height of incoming waves: 0.6 m to 1.2 m, peak period of incoming waves: 3.5 s to 8.0 s). The wave parameter were measured at 27 locations along the flume.

The numerical models HISWA, SWAN and MIKE 21 EMS were applied for the same bathymetry and boundary conditions. The three graphs at the top of Figure 1 show the significant wave height calculated by the numerical models in comparison to the wave height determined experimentally. Both physical and numerical modelling show a large decrease of wave height at the summer dike while the decline in the polder area is only very small. An increase of the significant wave height due to shoaling above the foreland can also be found in all models but the amount of increase seems to be underestimated by the numerical models HISWA and SWAN compared to the experiment. This may be contributed to the reflection of waves at the summer dike. The results of MIKE 21 EMS shown in figure 1 were averaged in wave direction using a running filter. The averaging is necessary since MIKE 21 EMS calculates the wave propagation only for regular waves. This leads to a standing wave directly in front of the summer dike which is not reasonable

for irregular waves. The filter width is chosen equal to the wave length of a regular wave with a period T_p.

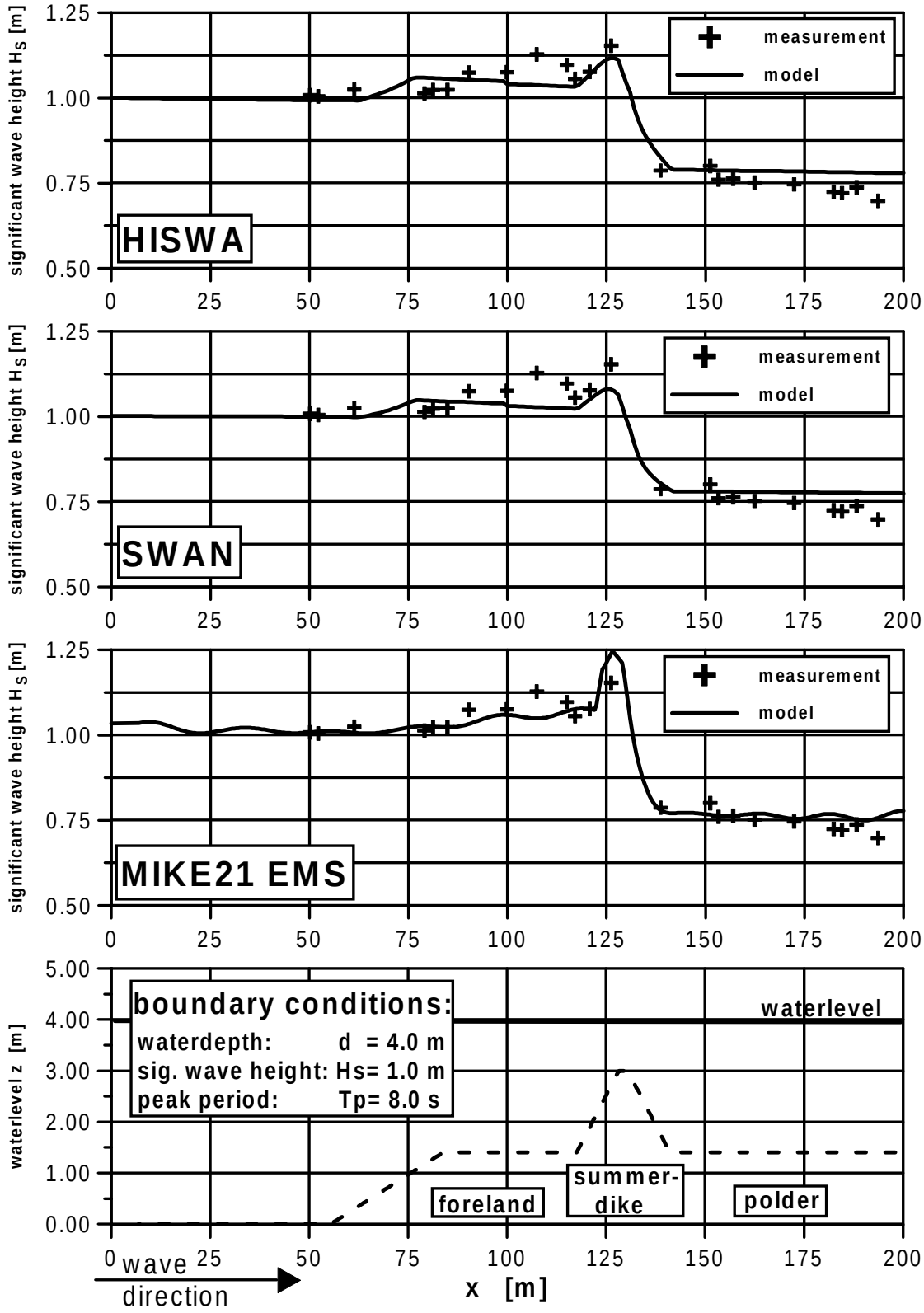

Figure 1 Comparison of the measured significant height of waves propagating in a wave tank with results of the models HISWA, SWAN, MIKE 21 EMS.

The parameters of the numerical models describing bottom friction and wave breaking were adjusted in order to give the best agreement of experimentally and numerically derived transmission coefficients of foreland and summer dike. The transmission coefficient is defined as

the quotient of the transmitted significant wave height $H^{trans}_{s(x=185m)}$ and the incoming significant wave height $H^{in}_{s(x=50m)}$:

$$c_T = \frac{H^{trans}_{S(x=185m)}}{H^{in}_{S(x=50m)}} \tag{15}$$

The best agreement was achieved using the model parameter listed in table 1.

Dissipation process	Numerical model		
	HISWA	SWAN	MIKE 21 EMS
Wave breaking	$\alpha = 0.95$ $\gamma_1 = 0.85$ $\gamma_2 = 0.95$	$\alpha = 1.45$ $\gamma = 0.75$	$\alpha = 1.0$ (not adjustable) $\gamma_1 = 1.05$ $\gamma_2 = 0.85$
Bottom friction	$C_{fw} = 0.01$ (using eq. 8)	K_N=0.02 (using eq. 9)	$K_N = 0.03$

Table 1 Optimised set of model parameters

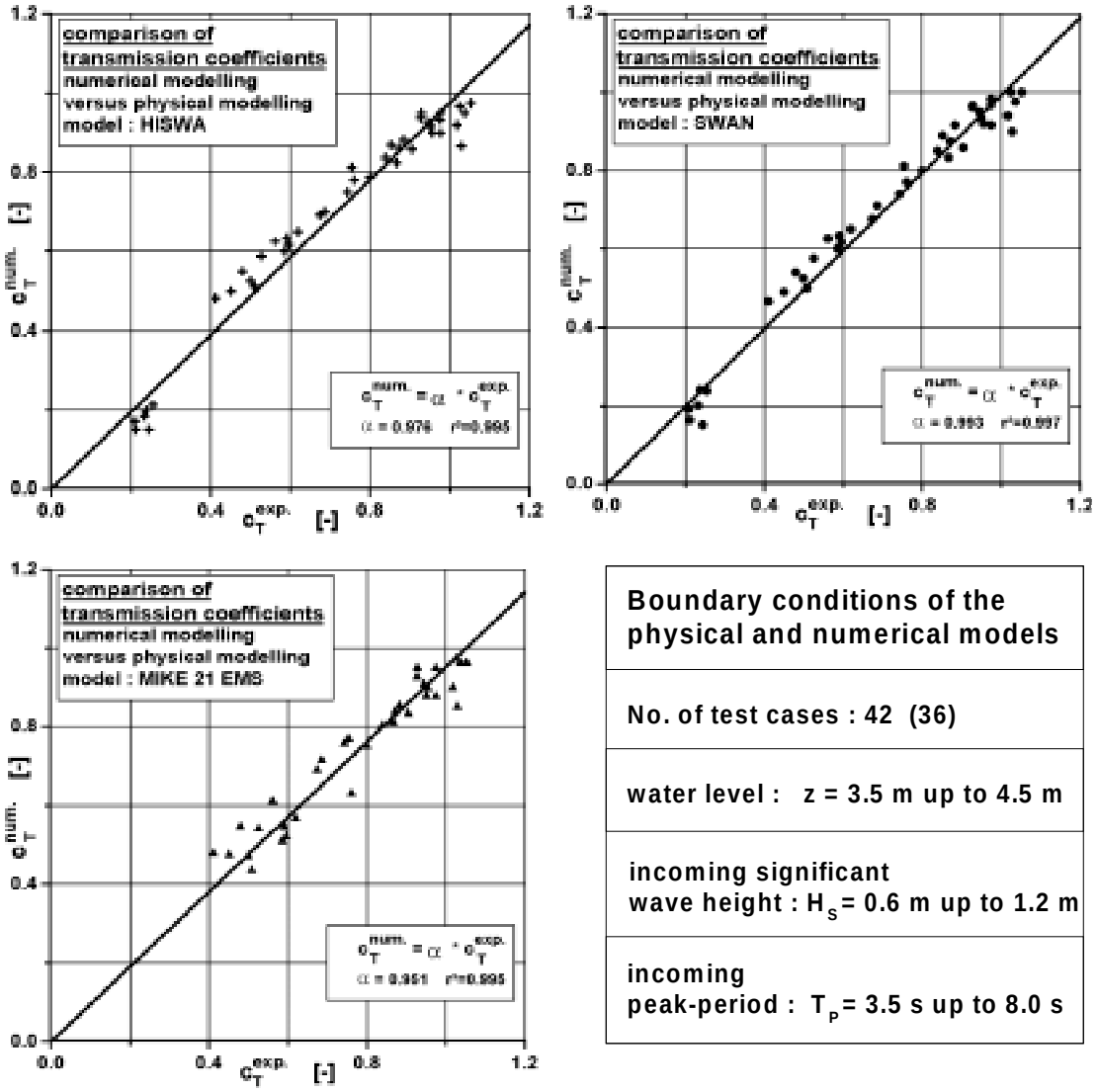

Figure 2 Comparison of the transmission coefficient calculated from the experiments in the wave flume $c_T^{exp.}$ with transmission coefficient calculated from numerical simulations $c_T^{num.}$ using the models HISWA, SWAN and MIKE 21 EMS

The transmission coefficients $c_T^{exp.}$ calculated from data acquired in the wave tank are compared with the transmission coefficients $c_T^{num.}$ calculated from numerical modelling using the optimised set of parameters (Figure 2). The experimental results are fitted well by all models. The best fit is found using SWAN with an average quotient of transmission coefficients of $\alpha = \frac{c_T^{num.}}{c_T^{exp.}} = 0.993 \approx 1$ and an explained variance of $r^2 = 0.997$.

4. NUMERICAL SIMULATIONS COMPARED TO FIELD DATA

The SWAN model test was performed within the wadden sea on the German North-Sea coast. The model area is situated between the North-Frisian island Pellworm and the peninsula Eiderstedt, as shown in figure 3. It contains the Hever tidal basin and a wide spread tidal inlet with shoals up to 2 m above MSL.

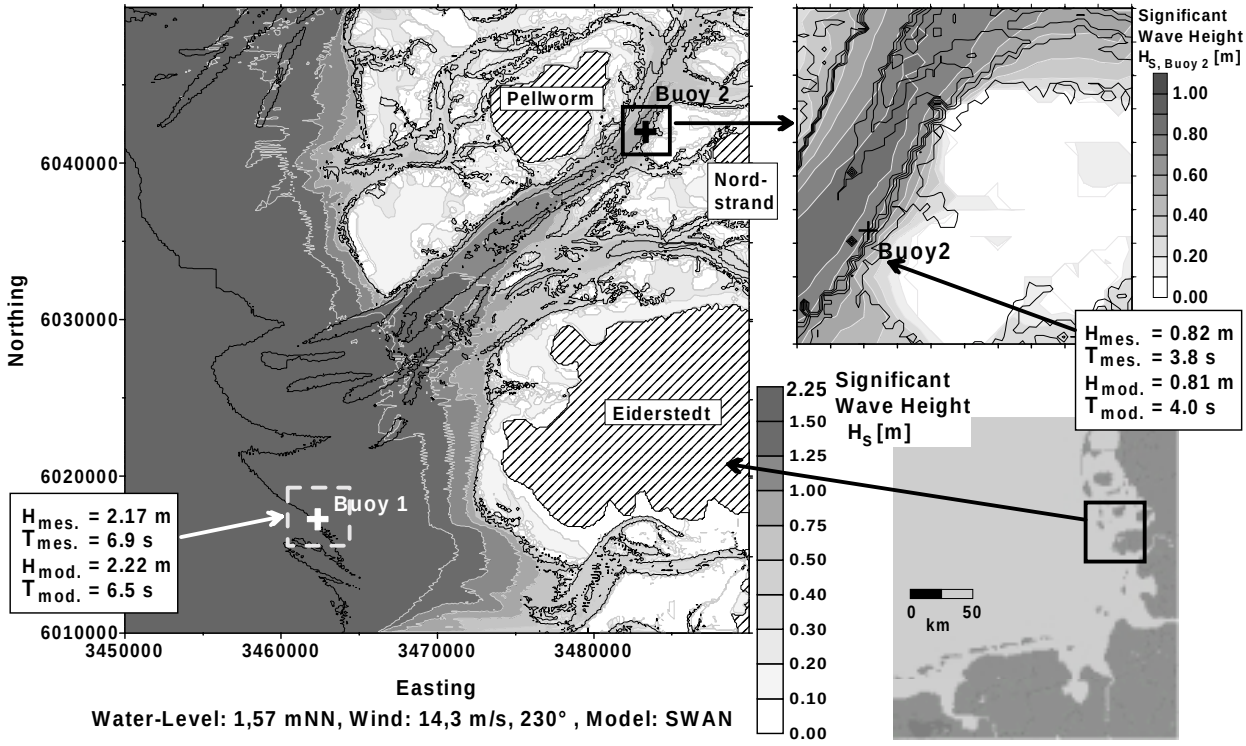

Figure 3 Comparison of the significant wave heights calculated by SWAN with those measured with two WAVERIDER buoys situated within the model area at the North-Frisian wadden sea coast of Germany

A data-set collected during field measurements carried out by the public department ALR Husum with two WAVERIDER buoys, one in the South located near the open sea and the other in the North sheltered by the island Pellworm, is used for the test of the numerical model SWAN. Besides the wave parameters the water-level and the wind conditions were measured. A detailed description and a survey of the wave parameter is given in Pabst (1998).

The complete data-set of wave measurements was reduced to a collective of 50 cases to be compared with SWAN simulations fulfilling the conditions of only slowly varying westerly wind

(the wind velocity should not vary more than 10 % two hours before the measurement of wave parameters). The numerical simulations of wave propagation were carried out using the measured boundary conditions, i.e. water-level and wind. The parameter of the incoming wave at the western seaward side of the model are set to be equal to the parameter measured at the position of buoy no. 1. An example of the wave-propagation and of the measured parameter is shown in figure 3.

A comparison of the calculated significant wave heights at the locations of buoy no. 1 and 2 and of the measured wave heights is given for the complete test collective in figure 4.

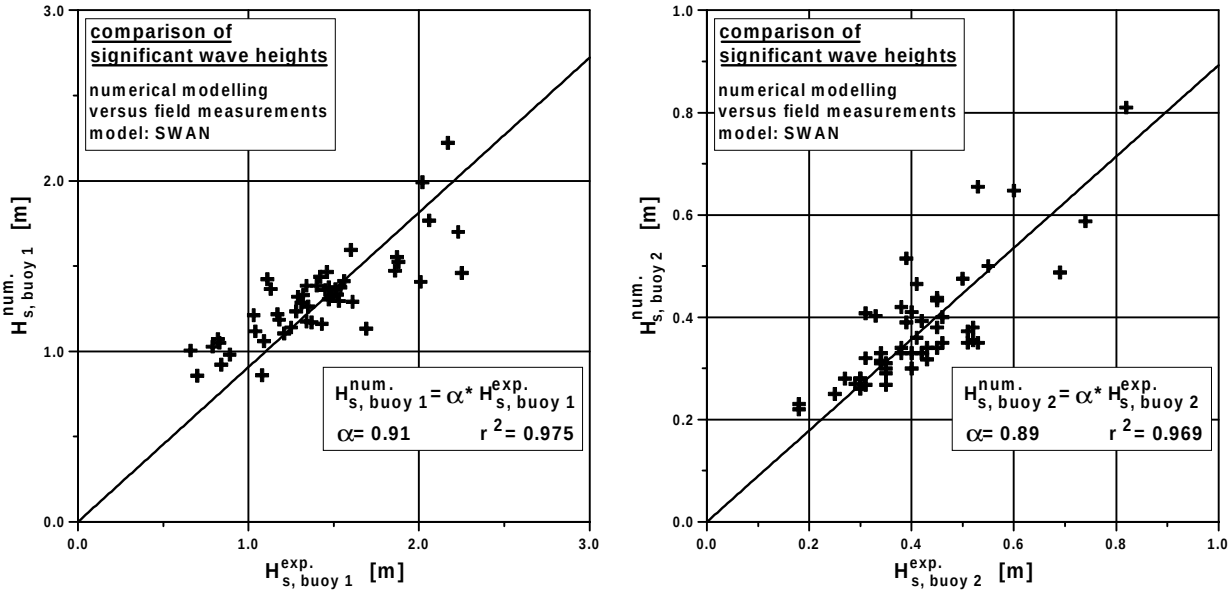

Figure 4 Comparison of the significant wave height obtained from field measurements and simulations with SWAN at the location of buoy no. 1 (left) and buoy no. 2 (right).

Even though the wave parameter measured at buoy no. 1 were used to prescribe the incoming wave field the significant wave height at the location of buoy no.1 is underestimated by the numerical simulations using the standard model parameters, especially in case of significant wave heights $H^{exp}_{s,buoy1} > 1.7$ m. This may be contributed to a too low energy input by wind generation. The average quotient of simulated and measured wave heights at buoy no. 1 is approximately $\alpha = 91\%$. At the location of buoy no. 2 the same underestimation of wave heights can be found, the average quotient of simulated to measured wave heights is $\alpha = 89\%$. But still a clear correlation of measurements and numerical simulations is evident. The correlation coefficient is approximately r^2=0.97. One reason for the scatter of modelled wave heights around measured heights may be the interaction of the tidal currents with the wave field.

5. CONCLUSION

The wave models HISWA, SWAN and MIKE 21 EMS are applicable very well for forecasts of the transmission coefficient at forelands and summer dikes. Best results in comparison with experimental wave tank data was achieved with model parameters of friction and wave breaking only slightly changed from the recommend values in the manuals.

The simulations of wave propagation in coastal shallow waters using SWAN revealed differences in wave height from measured data up to 30 %. These may be contributed in part to the influence of tidal currents on waves.

ACKNOWLEDGEMENT

We thank our colleague Dr.-Ing. K.-F. Daemrich for his support during the experiments in the wave tank and his contributions to the data analysis and interpretation.

REFERENCES

BATTJES, J.A. and J.P.F.M. JANSSEN (1978). Energy Loss and Set-up due to Breaking of Random Waves, Proc. 16th ICCE, Hamburg, pp. 569-587.

BOOIJ, N., HOLTHUIJSEN, L.H. and T.H.C. HERBERS (1985). A Numerical Model for Wave Boundary Conditions in Port Design, Int. Conf. on Numerical and Hydraulic Modelling of Ports and Harbours, Birmingham, pp. 263-268.

BOOIJ, N., HOLTHUIJSEN, L.H. and T.H.C. HERBERS (1985). The Shallow Water Wave Hindcast Model HISWA Part I: Physical and Numerical Background, Rep. No. 6-85.

COLLINS, J.I. (1972). Prediction of Shallow Water Spectra, J. Geophys. Res., 77, no. 15, pp. 2693-2707.

DANISH HYDRAULIC INSTITUTE DHI (1996). MIKE 21, Elliptic-Mild-Slope Wave Module, Release 2.6, User Guide and Reference Manual.

DINGEMANS, M.W. (1983). Verification of Numerical Wave Propagation Models with Field Measurements, CREDIZ Verification Haringvliet, Rep. W488, Part 1b, Delft Hydraulics, Delft.

Holthuijsen, L.H. and N. Booij (1987) A Grid Model for Shallow Water Waves, Proc. 20th ICCE, Taiwan, pp. 261-270.

KAISER, R. AND H.D. NIEMEYER (1998). Changing of Local Wave Climate Due to Ebb Delta Migration, 26th ICCE, Copenhagen

MADSEN, P.A. AND J. LARSEN (1987). An Efficient Finite-Difference Approach to the Mild-Slope Equation, Coastal Engineering, no. 11., pp. 329-351.

MADSEN, P.A., POON, Y.K. and H.C. GRABER (1988): Spectral Wave Attenuation by Bottom Friction: Theory, 21th ICCE, pp. 492-504.

MAI, S., DAEMRICH, K.-F. and C. ZIMMERMANN (1998). Wave Transmission at Summer Dikes, Wasser+Boden, no. 11, pp. 28-40 (original in German).

NIEMEYER, H.D. and R. KAISER (1998). Modeling of Effectiveness of Wave Damping Structures in Wadden Sea Areas, Proc. 5th Int. Workshop on Wave Hindcasting and Forecasting, Melbourne, Florida.

PABST, C. (1998). Wave Characteristics in Shallow Waters. Diploma Thesis, University of Hannover, (original in German, unpublished).

RIS, R.C., HOLTHUIJSEN, L.H. and N. BOOIJ (1994). A Spectral Model for Waves in the Near Shore Zone, 24th ICCE, Kobe ,pp. 60-70.

RIS, R.C. (1997). Spectral Modelling of Wind Waves in Coastal Areas, Communications on Hydraulic and Geotechnical Engineering, report no. 97-4, TU Delft.